Surfactant Organization in MCM-41 Mesoporous Materials As Studied by ^{13}C and ^{29}Si Solid-State NMR

Roberto Simonutti, Angiolina Comotti, Silvia Bracco, and Piero Sozzani*

Department of Materials Science, University of Milan-Bicocca, via R. Cozzi 53, I-20125 Milan, Italy

Received May 18, 2000. Revised Manuscript Received December 19, 2000

Mesoporous silica materials (MCM-41) were characterized by ^{13}C and ^{29}Si magic angle spinning (MAS) NMR. ^{13}C chemical shifts reveal a high content of gauche conformations in the chain of cationic surfactant molecules within the nanopores. ^{13}C T_1's and proton to carbon cross-polarization times (T_{CH}) demonstrate that the surfactant inside the pores exhibits anisotropic motions progressively reduced from the chain end toward the polar head. Variable-temperature ^{13}C MAS NMR spectra show a strong thermal dependence of the motions and highlight a gellike aggregation of the surfactant. On the other hand, the transfer of magnetization from the surfactant protons to the silicons on the pore surface was found to be efficient and observed by cross-polarization dynamics following the nonprotonated silicon atoms. Silicons and carbons receive magnetization from the same proton system, because a unique $T_{1\rho}(^1H)$ is measured from the point of view of silicon and carbon nuclei. Our results demonstrate that there is such an interaction between the ammonium group of the surfactant and the silica surface which represents a strong limit to the motion of the aliphatic chains.

Introduction

Interest in mesoporous materials has been growing fast in recent years, since the development of new synthetic routes based on the templating assembly of soluble inorganic species.[1,2] As a result of this interest, there has been a lot of literature dealing with the possibility of tuning the pore diameter on the nanometric scale[3,4] so as to form intrachannel clusters (metal, metal oxide, and semiconductor), to support catalysts, and to prepare new inclusion compounds.[5]

MCM-41 materials are silica-based systems possessing a uniform hexagonal array of cylindrical mesopores. The pore structure is due to the surfactant molecules which, in an aqueous solution, organize themselves in micelles and constitute a cast for the soluble silicates. After removal of the templating molecules by calcination, accessible mesopores are produced.

Until now, little characterization of the structure of surfactant molecules inside the MCM-41 channels has been reported. In any case this material can be viewed as a composite, with extended interfaces organized on the nanometric scale, and as an intriguing example of molecular confinement.

In the past we studied by solid-state NMR several examples of confined systems, where single alkanes or polymer chains are confined in 5 Å channels and show unusual conformational and dynamical properties.[6−9] The channels of MCM-41 systems, where the diameter ranges from 1.6 to 6 nm, allow the study of a micelle in the frozen state.

Also polymer/silica composites, materials with promising applications in the tire industry, are influenced by the interactions between the organic moieties and silica. Recently, we reported a ^{13}C and ^{29}Si magic angle spinning (MAS) NMR study of a polyisoprene (PI)/silica system,[10] where characterization of the cross-polarization (CP) dynamics allowed us to demonstrate the proximity between the polymer and the silica surface at the molecular level.

Therefore, the interaction between the surfactant and the silica walls of MCM-41 can be viewed as a nanostructured model of a more general silica/polymer adhesion.

Experimental Section

Synthesis of MCM-41. Mesoporous silica was synthesized using a cationic surfactant (S^+) for the structuring of positively charged inorganic species (I^+) through the presence of countercharged ions ($S^+X^-I^+$ mesostructure).[3,4] The surfactant used

* To whom correspondence should be addressed. E-mail: piero.sozzani@mater.unimib.it.

(1) Kresge, C. T.; Leonowics, M. E.; Roth, W. J.; Vartuli, J. C.; Beck, J. S. *Nature* **1992**, *359*, 710.
(2) Beck, J. S.; Vartuli, J. C.; Roth, W. J.; Leonowics, M. E.; Kresge, C. T.; Schmitt, K. D.; Chu, C. T.-W.; Olson, D. H.; Sheppard, E. W.; McCullen, S. B.; Higgins, J. B.; Schlenker J. L. *J. Am. Chem. Soc.* **1992**, *114*, 10834.
(3) Corma, A. *Chem. Rev.* **1997**, *97*, 2373.
(4) Huo, Q.; Margolese, D. I.; Ciesla, U.; Demuth, D. G.; Feng, P.; Gier, T. E.; Sieger, P.; Firouzi, A.; Chmelka, B. F.; Schüth, F.; Stucky, G. D. *Chem. Mater.* **1994**, *6*, 1176.
(5) Moller, K.; Bein, T. *Chem. Mater.* **1998**, *10*, 2050.
(6) Sozzani, P.; Bovey, F. A.; Schilling, F. C. *Macromolecules* **1989**, *22*, 4225.
(7) Sozzani, P.; Behling, R. W.; Schilling, F. C.; Bruckner, S.; Helfand, E.; Bovey, F. A.; Jelinski, L. W. *Macromolecules* **1989**, *22*, 3318.
(8) Sozzani, P.; Bovey, F. A.; Schilling, F. C. *Macromolecules* **1991**, *24*, 6764.
(9) Sozzani, P.; Amundson, K. R.; Schilling, F. C. *Macromolecules* **1994**, *27*, 6498.
(10) Simonutti, R.; Comotti, A.; Negroni, F.; Sozzani, P. *Chem. Mater.* **1999**, *11*, 822.

10.1021/cm001088i CCC: $20.00
Published on Web 02/27/2001

was cetyltrimethylammonium chloride (C_{16}TMACl; 98%, Fluka). Tetraethyl orthosilicate (TEOS; >99%, Fluka) was the silica precursor. To obtain a high content of surfactant in the silica MCM-41 composite, the synthesis was carried out with a surfactant weight concentration of 15% corresponding to the following molar ratio: 1.46:1:5.4:125.3 C_{16}TMACl/TEOS/HCl/H_2O. The surfactant was mixed with deionized water at 50 °C, then HCl (32% Fluka, 10 M) was added dropwise under vigorous stirring, and after 1 h TEOS was added. The solution was kept under stirring for 1 week, with deionized water being added (when necessary) to keep the composition of the mixture constant. The resultant material was filtered, washed repeatedly with deionized water, and allowed to dry at room temperature [sample MCM-41(A)]. Part of the sample was dried at 130 °C for 8 h under a nitrogen flux [sample MCM-41(T)]. Template removal was conducted by calcination in a muffle furnace at 630 °C for 5 h [sample MCM-41(C)].

Small-Angle X-ray Scattering (SAXS). SAXS diffraction patterns were recorded with a Kratky camera, using Cu Kα radiation at $\lambda = 1.5418$ Å. Intensity data were collected with a MBraun OED-50M position-sensitive detector between 0.1 and 5° (2θ) and were successively corrected for the blank scattering.

Nitrogen Adsorption. Nitrogen adsorption isotherms were measured at liquid nitrogen temperature using a Coulter SA 3100 analyzer. Samples were outgassed for 24 h at 100 °C. Surface areas were calculated using the BET model.

Thermogravimetric Analysis (TGA). The degradation and loss of the template molecules were evaluated using a Perkin-Elmer TGA-7 instrument. About 20 mg of MCM-41(A) was placed in a crucible and heated from room temperature to 650 °C at a heating rate of 20 K/min and a flow rate of 150 mL/min.

Solid-State NMR. High-resolution ^{13}C and ^{29}Si MAS NMR spectra were run at 75.5 and 59.6 MHz, respectively, on a Bruker MSL300 instrument operating at a static field of 7.04 T. A Bruker MAS probe was used with 7 mm ZrO_2 rotors; the spinning speed ranged between 2 and 4.5 kHz. Variable-temperature experiments were performed using a Bruker cooling system, in which only the bearing flux is cooled. Temperatures ranged between 275 and 358 K, and the stability was ±1 K. The experiments were made using a high-power proton decoupling (DD). ^{13}C CPMAS experiments were performed using a 90° pulse of 4.5 μs with a delay time of 4−10 s and a contact time ranging from 0.4 to 18 ms (DD field of 62 kHz). Experiments were run, collecting 200−400 scans. ^{29}Si CPMAS experiments were run using a 90° pulse of 6 μs with a delay time of 10 s, collecting 800−1000 scans (DD field of 42 kHz). ^{13}C single-pulse excitation MAS (SPE MAS) were performed using a recycle delay of 8 s; quantitative ^{29}Si SPE MAS experiments were recorded using a recycle delay of 100 s; 2000−3000 scans were collected. Longitudinal relaxation times, $T_1(^{13}C)$, were measured for each carbon under the CP condition; this was achieved by application of the pulse sequence developed by Torchia.[11]

Proton spin−lattice relaxation times in the rotating frame, $T_{1\rho}$ (^{1}H), were measured independently of ^{1}H → ^{13}C (or ^{29}Si) CP dynamics by varying the duration of a ^{1}H spin-lock period before a fixed ^{1}H → ^{13}C (or ^{29}Si) CP contact period.

The resolution for carbon was checked on glycine (full width at half-height = 22 Hz). Crystalline polyethylene was taken as an external reference at 33.63 ppm from tetramethylsilane (TMS).[12] The resolution for silicon was checked on a Q_8M_8 sample (trimethylsilyl ester of octameric silicic acid, $Si_8O_{20}H_8$). A Q_8M_8 sample was also used as a second standard, assigning the ^{29}Si chemical shift (CS) of the trimethylsilyl groups to +11.5 ppm from TMS.[13]

CP dynamics were determined through experiments with variable contact time, with the signal intensity being measured as a function of the contact time. The CP process allows the rare spin system S (^{13}C or ^{29}Si) to come into thermal contact with the neighboring system of abundant spins (protons) by means of a radio-frequency pulse sequence. In this sequence, the spin-locked (cold) system of abundant nuclei causes a large drop in the spin temperature of the rare nuclei system. Thus, there is a buildup of S magnetization. The buildup of S magnetization is ruled by the equation[14,15]

$$M(t) = \frac{M_0}{1 - \dfrac{T_{SH}}{T_{1\rho}(^1H)}}\{\exp[-t/T_{1\rho}(^1H)] - \exp[-t/T_{SH}]\} \quad (1)$$

where $T_{1\rho}(^1H)$ is the relaxation time of the proton nuclei in the rotating frame and T_{SH} the CP time. This equation is valid provided that the relaxation time of the rare nuclei in the rotating frame $T_{1\rho}(S)$ is much larger than $T_{1\rho}(^1H)$ and T_{SH}: a condition that is fulfilled in the case of rigid solids. Equation 1 describes two processes: the first exponential with time constant $T_{1\rho}(^1H)$ is the relaxation of the proton magnetization during the CP sequence; the other exponential, with the time constant T_{SH}, is the growth of the carbon (silicon) magnetization. When the Hartmann−Hahn condition is fulfilled, the inverse of the CP time $(T_{SH})^{-1}$ can be approximated as

$$(T_{SH})^{-1} = 1/2M_{2,SH}J_x$$

where $M_{2,SH}$ is the van Vleck second moment of the S spin resonance line determined by the dipolar coupling between the ^{13}C (^{29}Si) and ^{1}H nuclei and J_x the CP spectral density function of proton spins.[15] Considering that the second moment of the heteronuclear dipolar coupling at a first approximation varies as the inverse sixth power of the proton silicon distance, the CP time T_{SH} is proportional to the sixth power of the proton−rare nucleus distance. If the proton−rare nucleus distance is fixed (like in the case of protonated carbons), T_{SH} becomes mainly affected by the dependence of the J_x term on the mobility of the system in the kilohertz regime.

Results and Discussion

TGA, nitrogen absorption, and SAXS measurements allowed us to determine the MCM-41 characteristics of our samples. The calcined sample MCM-41(C) shows a BET surface area of 1185 m^2/g that is a typical value for mesoporous silicas.

The SAXS diffraction pattern of MCM-41(A) presents well-defined peaks corresponding to (100), (110), and (200) scattering reflections, confirming the formation of a hexagonal lattice with a pore diameter of ca. 43 Å (hexagonal with $a_0 = 2d_{100}/\sqrt{3}$). After the removal of the template by calcination (sample MCM-41(C)), the hexagonal structure is retained, but a decrease of the pore diameter to 34 Å is present; an analogous shrinkage of the channel upon calcination is described in ref 4. TGA gives an evaluation of the presence of the templating agent in the MCM-41(A) sample. At 280 °C the weight loss is about 43%, which is due to the decomposition of the cetylammonium residue and to the following combustion of the carbon species. The MCM-41(T) sample, treated at a temperature below the decomposition of the templating agent, behaves like sample MCM-41(A).

^{13}C NMR. ^{13}C CPMAS and SPE MAS NMR spectra of as-synthesized mesoporous silica MCM-41(A), still

(11) Torchia, D. A. *J. Magn. Reson.* **1978**, *30*, 613.
(12) Earl, W. L.; VanderHart, D. L. *J. Magn. Reson.* **1982**, *48*, 35.
(13) Lippmaa, E.; Mägi, M.; Samoson, A.; Engelhardt, G.; Grimmer, A. R. *J. Am. Chem. Soc.* **1980**, *102*, 4889.
(14) Mehring, M. *Principles of High-resolution NMR in solid in NMR Basic Principles and Progress*; Springer: Berlin, 1983; Vol. 12.
(15) Veeman, W. S.; Mass, W. E. J. R. *NMR Basic Principles and Progress*; Springer: Berlin, 1994; Vol. 32, p 129.

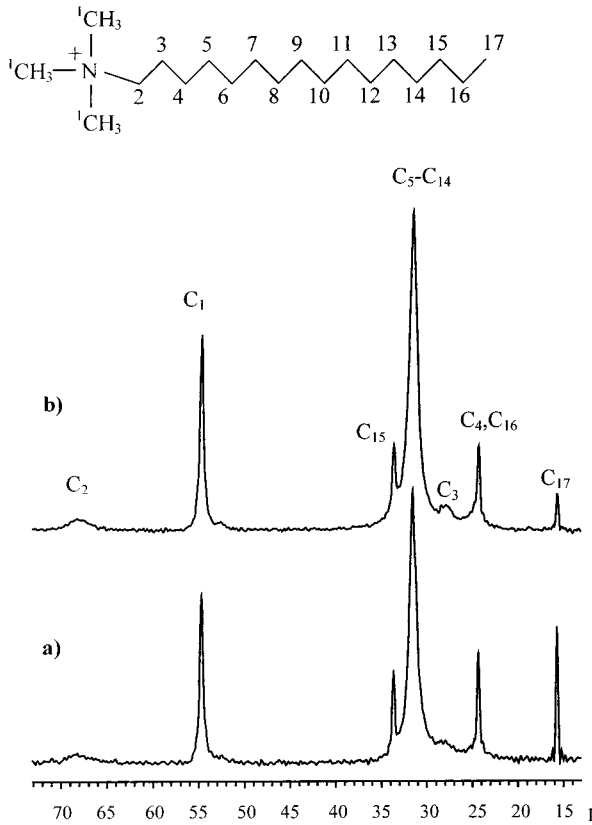

Figure 1. (a) 75.5-MHz ^{13}C SPE MAS spectrum of MCM-41-(A), with a spinning speed of 4000 Hz. A recycle delay of 10 s is applied. (b) 75.5-MHz ^{13}C CPMAS spectrum of MCM-41(A). A contact time of 2 ms is applied.

Table 1. ^{13}C δ (ppm) of Surfactant in Bulk and in Mesoporous Silica (Sample MCM-41(A))

carbon atom	MCM-41(A) solid ^{13}C δ (ppm)	C_{16}TAMCl	
		solid ^{13}C δ (ppm)	solution ^{13}C δ (ppm)
C_2	68.10	67.05, 64.55	66.80
C_1	54.66	54.61	53.41
C_{15}	33.59	36.40	31.92
C_5–C_{14}	31.55	34.70	29.44
C_3	28.48, 27.62	30.77, 29.19	26.24
C_4	24.64	27–24[a]	23.25
C_{16}	24.27	27–24[a]	22.68
C_{17}	15.60	18.22, 17.10, 16.56, 16.14	14.12

[a] Multiple peaks.

containing the templating agent, are depicted in Figure 1. No major differences between CP and SPE spectra are apparent, neither in terms of CS values nor considering the peak intensity (except for methyl C_{17}). The CS assignments are made by comparison to the solution spectrum[16] and are reported in Table 1. The resonance lines can be divided in two families: (a) a group of narrow lines due to the carbons along the chain (from C_5 to C_{16}), hereafter defined as midchain carbons, and to the methyls C_1 and C_{17}; (b) a family of broad peaks due to the carbons close to the polar group (from C_2 to C_4). Actually, the methylene carbon directly bonded to nitrogen presents a broad, hardly visible peak at 68.10 ppm: this behavior is typical of a carbon directly bonded to a nitrogen in the special case of restricted mobility.

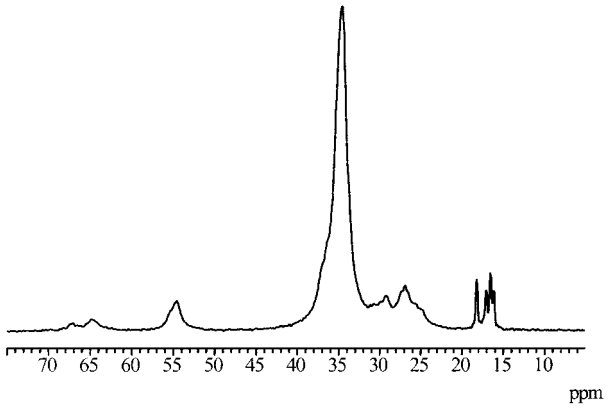

Figure 2. 75.5-MHz ^{13}C CPMAS spectrum of pure cetyltrimethylammonium chloride. A contact time of 2 ms is applied.

The broadening of the resonance is due to the ^{13}C–^{14}N dipolar coupling strongly affected by the ^{14}N quadrupole interaction.[17]

For comparison, the ^{13}C CPMAS NMR spectrum of the pure cetyltrimethylammonium chloride (as-received C_{16}TMACl) was recorded, shown in Figure 2. The spectrum is quite different from that in Figure 1 because some carbons present more than one resonance; e.g., the terminal methyl (C_{17}) produces four different CSs. Furthermore, the CS of the midchain methylenes is found at 34.70 ppm, while in the MCM-41(A) sample, the same methylenes resonate at 31.55 ppm with a 3.15 ppm upfield shift (Table 1). The terminal methyl of MCM-41(A) gives rise to a peak at 15.60 ppm slightly upfield, by 0.54 ppm, compared to the peak at highest field of the pure compound (16.14 ppm).

A lot of effort has been devoted to the ^{13}C MAS NMR characterization of linear alkanes in bulk[18,19] and in inclusion compounds.[6–9] the CS in the bulk phase has been assigned to the orthorhombic, triclinic, rotator, and melt phases; in the crystalline phases the chains assume a nearly all-trans conformation, and the CS of the inner methylenes ranges between 34.2 and 32.8 ppm,[20] depending on the reciprocal orientation of the zigzag planes and their state of motion; however, the melt phase is characterized by a large content of gauche conformations (estimated at about 35%) and shows a CS at 30.4 ppm; this value is in agreement with the estimated 5.3 ppm upfield shift for a full γ-gauche interaction.[21] Alkanes confined in the channels of inclusion compounds with a diameter of 5 Å assume, substantially, all-trans conformations endowed by motions. In a perhydrotriphenylene (PHTP) host, a fully aliphatic environment is provided to guest molecules, and the inner methylenes of hexadecane show a CS of 33.5 ppm;[22] however, the tris(*o*-phenylenedioxy)cyclophosphazene (TPP) host provides an aromatic environment to hexadecane and shifts the resonance to 32.1 ppm.[23]

(16) Bovey, F. A.; Mirau, P. A. *NMR of Polymers*; Academic Press: San Diego, 1996; p 42.

(17) Naito, A.; Ganapathy, S.; McDowell, C. A. *J. Chem. Phys.* **1981**, *74*, 5393.

(18) VanderHart, D. L. *J. Magn. Reson.* **1981**, *44*, 117–125.

(19) Möller, M.; Cantow, H. J.; Drotoll, H.; Emeis, D.; Lee, K. S.; Wegner, G. *Makromol. Chem.* **1986**, *187*, 1237.

(20) Ishikawa, S.; Kurosu, H.; Ando, I. *J. Mol. Struct.* **1991**, *248*, 361.

(21) Tonelli, A. *NMR Spectroscopy and Polymer Microstructure*: *The Conformational Connection*; VCH Publishers: Deerfield Beach, FL, 1988.

(22) Sozzani, P.; Simonutti, R.; Comotti, A. *Mol. Cryst. Liq. Cryst.* **1996**, *277*, 299.

In summary, the largest effect on the alkane ^{13}C CS comes from the conformation assumed by the chains; nevertheless, packing and susceptibility effects can play a nonnegligible role. The value of 34.70 ppm, found for the inner methylenes of C_{16}TMACl, is therefore in agreement with the chain in the all-trans conformation, while the chain-end methyls (C_{17}) present four conformations (four peaks from 16.14 to 18.22 ppm), due to trans and gauche conformations. A detailed NMR study of C_{16}TMACl will be published elsewhere.

In the MCM-41(A) sample, the aliphatic chains (excluding the polar heads that are grafted on the silica surface) interact mainly with each other; thus, the magnetic susceptibility for the inner methylenes does not change substantially, compared to the bulk phase. We therefore interpreted the upfield shift of 3.15 ppm (from 34.70 to 31.55 ppm) to be due to the exploration of gauche conformations, even if the gauche conformation fraction is lower than that in the melt phase. In fact, the conformational and diffusional freedom of the surfactant chains is reduced by two factors: (a) the channels of the mesoporous silica confine the chains in a restricted space; (b) the polar heads adhere to the inner silica surface and represent an anchor that blocks the free motion of the molecule. The ammonium group strongly interacts with the silica polar surface so its mobility is greatly reduced, as highlighted by the broadening of CH_2 in the α position to the ammonium moiety (C_2). Also the β and γ methylenes (C_3 and C_4) suffer from this restraint, presenting broad resonances in the MAS NMR spectrum. In the CPMAS spectrum the resonance of the C_3 unit is better defined and resolved in two peaks at 28.48 and 27.62 ppm; the C_4 signal in both spectra is a barely visible peak, partly overlapping with the sharp signal of the C_{16} unit.

Whenever incoherent molecular motion occurs on the same time scale as the introduced coherent averaging mechanism (high-power DD), the efficiency of the coherent averaging is reduced.[24] Therefore, motions of hundreds of microseconds of correlation time can reduce the effect of the dipolar decoupling; this effect is usually defined as motional broadening and can be overcome by performing variable-temperature NMR experiments.

Variable-temperature CPMAS spectra of MCM-41(A) are shown in Figure 3. Above room temperature there is an overall sharpening of the resonances, and at 358 K the line width of the peaks is comparable to that of a melt. Spectra run below room temperature reveal a considerable broadening of the peaks, and at 275 K only the resonance due to the methyl at the end of the long aliphatic chain (C_{17}) presents a narrow peak. At low temperature there is no evidence of crystallization; in fact, the CS of the inner methylenes does not change and still presents a large content of gauche conformations. This behavior confirms the hypothesis that the surfactant chains in the mesoporous channels are in an intermediate regime of motion at room temperature. At high temperature their mobility becomes close to that of aliphatic chains in solution or in a true melt; however, at low temperature decreased mobility leads to a general motional broadening of all of the peaks.

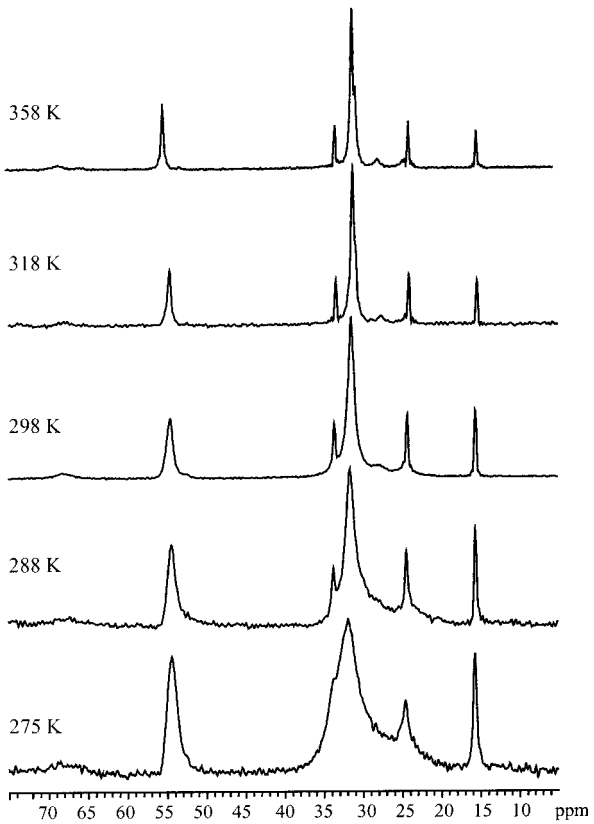

Figure 3. 75.5-MHz ^{13}C SPE MAS spectra of MCM-41(A) at variable temperatures ranging from 275 to 358 K. Spectra are collected with a relaxation delay of 10 s.

Table 2. ^{13}C T_1 and $^1H-^{13}C$ CP Time of Surfactant in Mesoporous Silica (Sample MCM-41(A))

carbon atom	chemical shift (ppm)	^{13}C T_1 (s)	$T_{1\rho}(^1H)$[a] (ms)	T_{CH} (ms)
C_2	68.10	0.13	*b*	*b*
C_1	54.66	0.16	4.1	1.4
C_{15}	33.59	0.56	6.5	0.5
C_5-C_{14}	31.55	0.40	4.5	0.5
C_3	28.48−27.62	0.30	*b*	*b*
C_4	24.64	*b*	*b*	*b*
C_{16}	24.27	0.72	7.3	1.9
C_{17}	15.60	>1	7.9	8.4

[a] $T_{1\rho}(^1H)$ was measured by transferring the magnetization to the carbon nuclei. [b] Value not determined.

^{13}C T_1's, measured at room temperature, are very short (Table 2) for all of the carbons of the MCM-41(A) sample. The main pathway of relaxation for the aliphatic carbon atoms is considered to be the dipolar relaxation to the directly bonded hydrogens.[25] Theoretical models demonstrated that, in the case of the dipolar mechanism, the T_1 relaxation times are at a minimum of about 0.1 s for motions with a correlation time of nanoseconds (considering Larmor frequencies between 50 and 125 MHz); thus, toward faster or lower motion frequencies, T_1 increases. In fact, both liquids (fast motion limit) and crystalline solids (slow motion limit) present long T_1's. To find a short T_1, it is necessary to consider either gels or amorphous polymers well above the glass transition. Very short ^{13}C T_1's demonstrate that the surfactant molecules in MCM-41(A) are characterized by this intermediate regime of motions. Fur-

(23) Comotti, A.; Simonutti, R.; Catel, G.; Sozzani, P. *Chem. Mater.* **1999**, *11*, 1476.
(24) White, J. L.; Dias, A. J.; Ashbaugh, J. R. *Macromolecules* **1998**, *31*, 1880.
(25) Menger, E. M.; Veeman, W. S.; de Boer, E. *Macromolecules* **1982**, *15*, 1406.

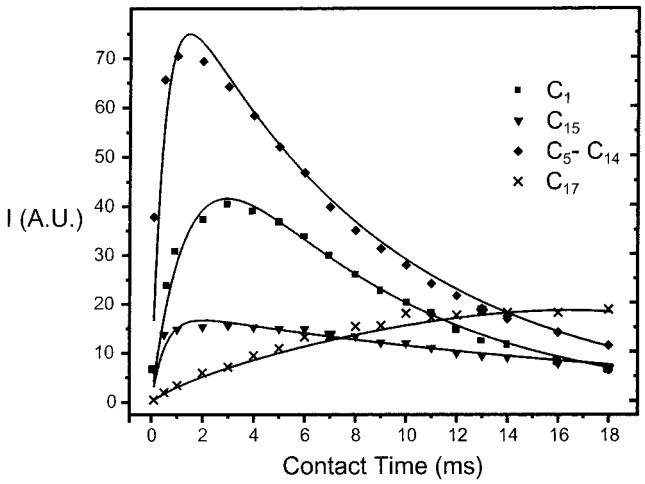

Figure 4. Evolution of ^{13}C magnetization in a variable contact time CP experiment and nonlinear least-squares fitting for selected carbon nuclei in MCM-41(A). The spectra are performed at room temperature.

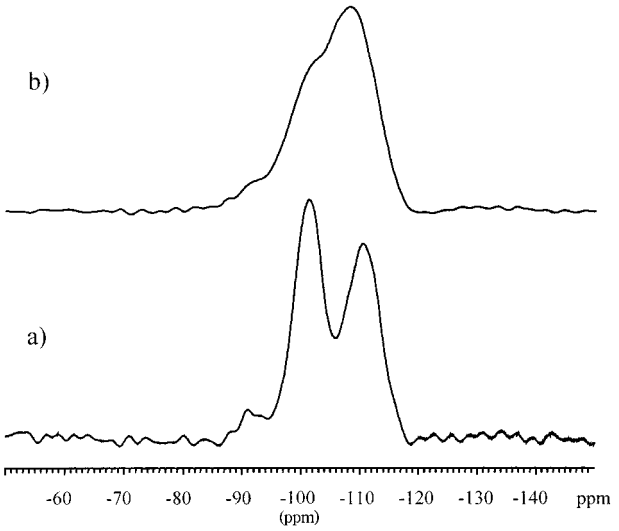

Figure 5. (a) 59.6-MHz ^{29}Si SPE MAS spectrum of MCM-41-(A). (b) 59.6-MHz ^{29}Si SPE MAS spectrum of calcined MCM-41(C). Spectra are collected with a relaxation delay of 100 s.

thermore, there is a smooth decrease of the T_1 values moving from the chain-end methylenes (0.72 s for C_{16}) to the methylenes close to the polar head (0.30 s for C_3); this behavior can be explained by progressively diminishing methylene mobility about single bonds. Methyl groups and the methylene carbon directly bonded to the nitrogen are not considered, with their relaxation being affected also by mechanisms other than dipolar relaxation.

As shown in Figure 1, the CPMAS technique is efficient on the MCM-41(A) sample; therefore, CP dynamics were exploited using variable contact time experiments. The CP curves of selected carbon atoms are depicted in Figure 4; values of T_{CH} are reported in Table 2. The exponential increase in the signal intensity with the time constant T_{CH} describes the transfer of polarization from the abundant ^1H spin reservoir to the dilute ^{13}C spin reservoir (see the Experimental Section). The value of T_{CH} is determined by the static dipolar coupling between the carbon and proton spins in the presence of a radio-frequency field of a few tens of kilohertz. Motions in the kilohertz regime can partly average the static dipolar interaction, increasing the value of T_{CH}.[26] In rigid systems protonated carbons usually present T_{CH} values of tenths of milliseconds, whereas in highly mobile systems T_{CH} can be so long that it is practically impossible to record a spectrum. In the case of MCM-41(A), a relatively short T_{CH} for the central methylenes demonstrates that the $^1H-^{13}C$ dipolar interaction is not completely averaged, and the chains present a limited mobility in the kilohertz regime. In fact, the actual motions in the system must not be isotropic but restricted by both the small volume available and the presence of a grafting point like the ammonium group. Longer T_{CH} values for the end groups (C_{16} and C_{17} units) are coherent with the higher mobility of these moieties as shown by the T_1 values.

^{29}Si NMR. $^1H-^{29}Si$ CP dynamics are a valuable tool for studying the proximity of macromolecular chains to silica and silicate surfaces. As we have recently demonstrated, it is possible, in the case of PI/silica composites,[10] to have transfer of magnetization from the protons of PI to the silicons at the silica surface. The same phenomenon allowed us to study the adhesion of poly(vinyl alcohol) at the heterogeneous interface with condensating silicates in hydrated cement pastes.[27]

The MCM-41(A) sample still containing cetyl chains is a nanostructured analogue of an extended polymer/silica surface. The pore structure of the silica confines the aliphatic chains in a restricted environment where the polar groups provide a grafting point at the organic–inorganic interface.

The ^{29}Si SPE MAS spectra of MCM-41(A) and MCM-41(C) are shown in Figure 5; 100 s of recycle delay was applied for a complete relaxation of the silicon nuclei. In the spectrum of MCM-41(A) (Figure 5a), two peaks are recognized: one, at −99 ppm, is assigned to silicon atoms bearing one hydroxyl group $(Si-O)_3Si-OH$ (single silanols called Q^3);[13] the other, at −109 ppm, is due to silicon atoms without hydroxyl groups $Si(Si-O)_4$ (called Q^4). The areas of the Q^4 and Q^3 peaks are nearly the same. A minor peak, at −89 ppm, is related to the presence of geminal silanols $(Si-O)_2Si-(OH)_2$ (called Q^2). In the case of MCM-41(C) (Figure 5b), the signals are broader and partially overlap; the Q^4 signal is more intense than the same resonance in the case of the MCM-41(A) sample.[28] The Q^3 and Q^2 species are present at the surface of the silica particle; thus, the intensity ratio $(Q^3 + Q^2)/Q^4$ is associated with the surface area of the silica; a decrease in this intensity ratio from the as-synthesized sample (MCM-41(A)) to the calcined one (MCM-41(C)) confirms that the calcination causes the partial condensation of the silanolic groups and the shrinkage of the channels, in agreement with the SAXS measurements. The broadening of the lines in the calcined sample is also related to the shrinkage, which determines a distortion of the siloxanic tetrahedra and an inhomogeneous broadening.[29]

(26) Silvestri, R. L.; Koenig J. L. *Macromolecules* **1992**, *25*, 2341.

(27) Comotti, A.; Simonutti, R.; Sozzani, P. *Chem. Mater.* **1996**, *8*, 2341.

(28) Hansen, E. W.; Schmidt, R.; Stöcker, M.; Akporiaye, D. *J. Phys. Chem.* **1995**, *99*, 4148.

(29) Sindorf, D. W.; Maciel, G. E. *J. Am. Chem. Soc.* **1983**, *105*, 1487.

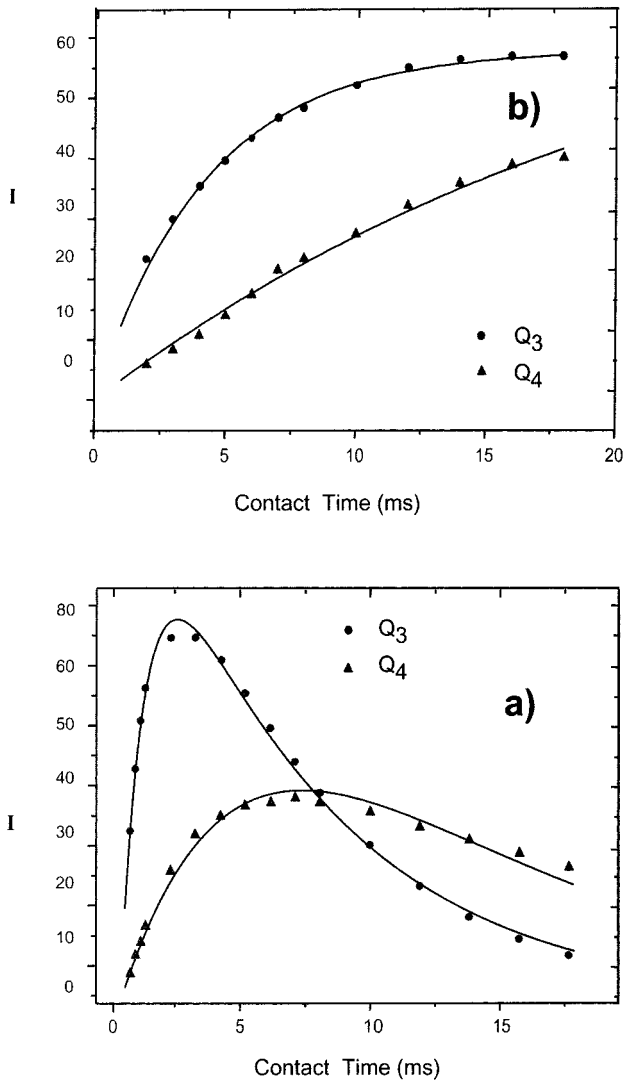

Figure 6. Evolution of ^{29}Si magnetization in a variable contact time CP experiment and nonlinear least-squares fitting for (a) MCM-41(A) and (b) calcined MCM-41(C): Q^3, filled dots; Q^4, filled triangles. The spectra are performed at room temperature.

Table 3. ^{1}H−^{29}Si CP Times and $T_{1\rho}(^1$H) Measured by Transferring the Magnetization to the Silicon Nuclei of MCM-41(A) and MCM-41(C)

sample	peak	T_{SiH} (ms)	$T_{1\rho}(^1$H) (ms)	magnetization (%)
MCM-41(A)	Q^3	1.0	6.8	66
	Q^4	7.1	7.4	34
MCM-41(C)	Q^3	4.2	25.7	46
	Q^4	22.3	23.4	54

The curves representing the fitting of the peak intensities of MCM-41(A) and MCM-41(C) samples from the variable contact time experiments are reported in parts a and b of Figure 6, respectively. The fitting was performed according to eq 1, using as a fixed parameter the independently measured values of $T_{1\rho}(^1$H). $T_{1\rho}(^1$H), T_{SiH}, and M_0 values are reported in Table 3. The calcined sample MCM-41(C) presents T_{SiH} and $T_{1\rho}(^1$H) values of the same order of magnitude as those reported for various silicas.[30,31] In pure siliceous systems, Q^3 groups, having a proton two bonds apart, show short T_{SiH}; on the contrary, the Q^4 silicons have rather long T_{SiH} because they are not in close contact with protons and can receive magnetization only from the protons of single or geminal silanol groups which are at least four bonds apart. Q^4 and Q^3 show the same long $T_{1\rho}(^1$H) because the reservoir of proton magnetization is the same for both of the silicon atoms (the surface hydroxyls and the hydrogen-bonded water). Untreated silicas usually present values of $T_{1\rho}(^1$H) of tens of milliseconds. In the MCM-41(A) sample containing the surfactant chains, an overall shortening of the values of T_{SiH} and $T_{1\rho}(^1$H) is evident, as was also reported by Steel et al.[32]

The presence of the surfactant molecule makes it possible to measure the $T_{1\rho}(^1$H) of the proton reservoir associated with the organic molecule, transferring the proton magnetization to the carbon nuclei. The $T_{1\rho}(^1$H) values measured in this way are reported in Table 2; the average value of 6 ms is close to that measured by transferring the proton magnetization to the silicon nuclei (7 ms).

In our opinion, the CP behavior for the MCM-41 material containing the surfactant molecules can be discussed by taking into account the model proposed by Maciel and co-workers for a silica surface.[33] The surface of amorphous silica can be represented on the scale of a few nanometers as an alternation of shreds of the hydroxylated (100) and (111) surface of β-cristobalite. The (100) surface is characterized by geminal silanols; however, the (111) surface presents rows of single silanols. In the case of MCM-41, the channel structure determines a surface with some degree of curvature, which anyway does not change drastically the local geometry of the silicon tetrahedra; in fact, the values of CS for Q^3 and Q^4 are compatible with the values reported for the usual silicas. On the (111) face of cristobalite, the silanols are at a distance of 5 Å[34] and water molecules form a bridge between two adjacent silanols via hydrogen bonding, determining a reduction of the O−H mobility. Decreased mobility means stronger ^{1}H−^{29}Si dipolar interaction; thus, Q^3 peaks in hydrated silicas show shorter T_{SiH} than those in silicas where the adsorbed water is removed. For what concerns the Q^4 species, the water hydrogen-bonded to silanols buries these species, preventing the possibility that other water molecules can be absorbed near them, determining a quite long value of T_{SiH}.

In the case of MCM-41(A) containing the surfactant molecules, a part of the water is substituted by the polar heads of the surfactant and the trimethylammonium group strongly interacts with the charged silica surface, as demonstrated by Chmelka and co-workers[35,36] using two-dimensional heteronuclear correlation NMR measurements. Therefore, the methyls of the polar head can come close to the Q^4 atoms, as confirmed by the great

(30) Pfeiderer, B.; Albert, K.; Bayer, E.; van de Ven, L.; de Haan, J.; Cramers, C. *J. Phys. Chem.* **1990**, *94*, 4189.
(31) Leonardelli, S.; Facchini, L.; Fretigny, C.; Tougne, P.; Legrand, A. P. *J. Am. Chem. Soc.* **1992**, *114*, 6412.
(32) Steel, A.; Carr, S. W.; Anderson, M. W. *Chem. Mater.* **1995**, *7*, 1829.
(33) Chuang, I.-S.; Maciel, G. E. *J. Am. Chem. Soc.* **1996**, *118*, 401.
(34) Ceresoli, D.; Bernasconi, M.; Iarlori, S.; Parrinello, M.; Tosatti, E. *Phys. Rev. Lett.* **2000**, *84*, 3887.
(35) Janicke, M. T.; Landry, C. C.; Christainsen, S. C.; Kumar, D.; Stucky, G. D.; Chmelka, B. F. *J. Am. Chem. Soc.* **1998**, *120*, 6940.
(36) Janicke, M. T.; Landry, C. C.; Christiansen, S. C.; Birtalan, S.; Stucky, G. D.; Chmelka, B. F. *Chem. Mater.* **1999**, *11*, 1342.

reduction of T_{SiH} in the MCM-41(A). A relevant reduction of T_{SiH} for the Q^4 peak was also measured in the case of a PI/silica composite,[10] when the activity of a bidentate grafting agent ensured the proximity of the polymer protons to the silica surface within a few angstroms. The $T_{1\rho}(^1H)$ values measured transferring proton magnetization to carbons and silicons are practically the same and much shorter than those measured for the calcined sample. This is a clear suggestion that silicon and carbon nuclei receive magnetization from the same ensemble of protons mainly constituted by the surfactant protons. Furthermore, the efficient $^1H \rightarrow {}^{13}C$ magnetization transfer found for the carbon atoms of the surfactant chain close to the ammonium group confirms that this portion of molecule presents restricted anisotropic motions.

Conclusions

High-resolution solid-state NMR observations, from the viewpoint of both ^{13}C and ^{29}Si, allowed us to describe the mobility and the conformation of the C_{16}TMACl molecules confined in MCM-41 channels with a diameter of 43 Å. ^{13}C CS values showed that the main chain explores a great number of gauche conformations. Peak line widths and carbon T_1's highlight a marked mobility of the tail of the aliphatic chain; however, methylene units near the ammonium group present a reduction of motion. This result is confirmed by $^1H \rightarrow {}^{13}C$ and $^1H \rightarrow {}^{29}Si$ CP dynamics, where relatively short T_{CH} for central methylenes of the surfactant and unusually short T_{SiH} for Q^4 species are found. Silicons and carbons receive magnetization from the same proton system, because a single $T_{1\rho}(^1H)$ is measured from the point of view of silicon and carbon nuclei, confirming the close proximity of the surfactant molecule to the silica surface.

The literature usually reports a simple model for MCM-41 materials containing surfactants: this describes C_{16}TMACl molecules within the MCM-41channels as a regular array of extended chains. The present data contribute to the definition of a more realistic picture of the chains confined in mesoporous materials. Our model takes into account the conformational disorder of the aliphatic chain and the specific interaction between the ammonium group and the pore surface. On the other hand, composites and nanocomposites derive their properties (mechanical, electrical, and transport properties) from the interaction between an inorganic filler and a polymer matrix. Organic−inorganic interfaces are thus the key point to be addressed, but a molecular description of the heterogeneous interphase is difficult because usually it is present in a small quantity and shows high complexity. MCM-41 silica systems with extended and structured interfaces provide a model for surfactant/silica interphases and polymer/silica composites.

Acknowledgment. Financial support from the Italian Ministry of University and Scientific Research (PRIN program) is gratefully acknowledged. We thank Prof. A. Marigo for the SAXS measurements.

CM001088I